Optics Communications 100 (1993) 331–340
North-Holland

OPTICS
COMMUNICATIONS

Full length article

Chaotic properties of the coherence collapsed state of laser diodes with optical feedback

C. Masoller, A.C. Sicardi Schifino and C. Cabeza
Instituto de Fisica, Facultad de Ciencias, T. Narvaja 1674, Montevideo, Uruguay
and Instituto de Fisica, Facultad de Ingeniera, Herrera y Reissig 565, Montevideao, Uruguay

Received 7 May 1992; revised manuscript received 21 January 1993

The characterization of the geometrical and statistical properties of the coherence collapsed state of laser diodes with optical feedback is done by means of dimension analysis and the spectrum of Lyapunov exponents. The dimension calculation evidences the fractal and low-dimensional structure of the attractor, while the spectrum of Lyapunov exponents unambiguously confirms the chaotic nature of the coherence collapsed state. In addition, we investigated the transition from quasiperiodicity to chaos as the feedback parameter was increased. The detection by Poincaré section analysis and power spectrum of three-period doubling bifurcations of a two-dimensional torus is presented.

1. Introduction

In recent years, optical feedback has become a fascinating subject from both the applied and the fundamental points of view. From the experimental point of view, optical feedback from an external cavity is commonly employed to reduce the linewidth of semiconductor lasers, in order to meet the requirements for the realization of coherent transmission systems and interferometric fiber sensors. From the theoretical point of view, optical feedback provides a good example of bifurcations and transitions to chaos in nonlinear physical systems.

In a computer simulation, Ikeda et al. [1] studied the behavior of transmitted light from a ring cavity containing a nonlinear dielectric medium and were the first to show that the presence of a time delay in the feedback loop might cause the laser to switch to a state of significantly increased phase and dynamical complexity. This coherence-collapsed state [2] has been interpreted as a chaotic attractor. Since then, chaotic behavior has been reported for many similar systems. For the external cavity laser diode, chaotic behavior has been observed both theoretically and experimentally [3–7].

Using the model of Lang and Kobayashi [8,9], Tromborg et al. recently showed [10,11] that the system undergoes a quasiperiodic route to chaos that can be interrupted by frequency locking. Even though the practical importance of this phenomenon, the chaotic properties of the coherence collapsed state are not quantitatively understood yet.

Although there are several results indicating that the attractors of infinite-dimensional systems are of finite dimension and have a discrete spectrum of Lyapunov exponents [12], only little is known about their structure and their behavior as the parameters are varied. In this letter the evolution and characterization of the coherence collapsed state is studied computing the dimension and the Lyapunov exponents, for the first time we believe.

The spectrum of Lyapunov exponents [13–17] provides a summary of the local stability properties of an attractor. The standard approach of Benettin et al. [13] and Shimada et al. [16], linearizing the equations of motion, was used to calculate the spectrum of Lyapunov exponents, and the largest Lyapunov exponent was also estimated studying the evolution of an infinitesimal perturbation at a given point on the attractor. The difference between both calculations gives an estimation of the accuracy in the Lyapunov exponents calculations. As the feedback parameter was increased, from the spectrum of Lyapunov exponents three period-doubling bifur-

cations of the two-torus were found before the transition to the chaotic state.

In order to investigate the dimension of the attractor, the method of delays [18–20] was employed to reconstruct the dynamics in a finite dimensional space. The correlation dimension of the coherence collapsed state, computed with the method of Grassberger and Procaccia [21], was found to be $D_c \approx 3.85$, while the Lyapunov dimension, computed according to the conjecture of Kaplan and Yorke [12,22,23], gives a value $D_L \approx 3.95$.

The detection by Poincaré section analysis and power spectrum of three period-doubling bifurcations of the torus is presented. This result agrees with whose of refs. [24,25], i.e. that period-doubling bifurcations of two-torus occur only a finite number of times before the system undergoes a transition to chaos.

This paper is organized as follows. Section 2 presents a brief discussion of the model and its main characteristics. In sec. 3 we investigate the transition to the coherence collapsed state by Poincaré and power spectrum analysis. The calculation of the spectrum of Lyapunov exponents is presented in sec. 4, while the dimension calculation is presented in sec. 5. Finally, sec. 6 is devoted tc the discussion of the results.

2. The model equations

The theoretical investigations of the external cavity configuration are usually based on the model of Lang and Kobayashi [8]. In this model the system is described by a set of coupled rate equations for the complex electric field $E(t)$ and the carrier density $N(t)$. The equations are nonlinear and the field equation contains a time-delayed term that accounts for the field reflected from the external mirror and that renders the system infinite dimensional. By separating the field equation into two equations for the amplitude $E(t)$ and the phase $\phi(t)$ we obtain the following set of equations

$$\mathrm{d}E(t)/\mathrm{d}t = \tfrac{1}{2}[G(N) - 1/\tau_p]E(t) + (k/\tau_{in})E(t-\tau)\cos\Delta(t)\,, \quad (1)$$

$$\mathrm{d}\phi(t)/\mathrm{d}t = \tfrac{1}{2}\alpha[G(N) - 1/\tau_p] - (k/\tau_{in})[E(t-\tau)/E(t)]\sin\Delta(t)\,, \quad (2)$$

$$\mathrm{d}N(t)/\mathrm{d}t = J - N(t)/\tau_s - G(N)E(t)^2\,, \quad (3)$$

where $\Delta(t) = \omega_0\tau + \phi(t) - \phi(t-\tau)$ is the phase delay, ω_0 being the angular frequency of the solitary laser; $G(N) = G_N(N - N_0)$ is the gain per unit time. τ_{in} and τ are the round-trip time in the laser cavity and the external cavity, respectively. k^2 is the feedback power ratio, i.e., is the power reflected from the external cavity relative to the power reflected from the laser mirror. α is the linewidth enhancement factor; τ_s is the carrier lifetime and J is the bias current. Equations (1)–(3) do not include multiple reflection, and are therefore valid only for $k \ll 1$.

In order to investigate the evolution of the system, we have done a numerical simulation. The equations were solved by a standard six-order Runge–Kutta integration routine, where the time increment was taken as $\Delta t = 0.02$ ns. The parameters used are: $\alpha = 6$, $G_n = 1.1 \times 10^{-12}$ m^3/s, $N_0 = 1.1 \times 10^{24}$ m^3, $\tau_s = 2$ ns, $\tau_p = 2$ ps, $\tau_{in} = 8$ ps and $\tau = 2$ ns. J was taken as $J = 2.0 J_{th}$, where J_{th} is the threshold current ($J_{th} = N_{th}/\tau_s$, $G(N_{th}) = 1/\tau_p$).

Let us now describe briefly the changes that occur in the nature of the system's attractor as the feedback k is increased. A linear stability analysis [9] shows that, for low values of k, the external cavity mode (ECM) with minimum carrier density is a stable fixed point of eqs. (1)–(3). The computer program was initiated from this fixed point, and was first started for the laser diode without feedback. Increasing k, we found that the ECM becomes unstable and a stable limit cycle appears. If we continue to increases k, this limit cycle looses stability and it is replaced by a two-torus, which period doubles three times and becomes chaotic.

In order to distinguish periodic behavior from chaotic behavior, we used a variety of methods [20]. Let us begin with two of the most commonly employed, namely the Poincaré section and the power spectrum [23,26].

3. Visualization of the dynamics

The solution describes a trajectory in (E, N, Δ)

space. For the visualization of the dynamics we used the Poincaré section technique, which easily allows the recognition of two-torus and its bifurcations. We plotted the normalized photon number $(I(t)/I_s = E(t)^2/E_s^2)$ and the phase delay $(\phi(t)-\phi(t-\tau))$ at the intersection points of the trajectory with the plane $N/N_{th}-1=0$; N_{th} and I_s corresponding to the solitary laser. Let us next present our results.

Increasing k, the first Hopf bifurcation occurs when the ECM becomes unstable and a limit cycle with oscillation frequency $f_0=5.77$ GHz is born. The limit cycle leads to a single intersection point in the Poincaré map [28] ("mirror" points are rejected). If we continue increasing k, this limit cycle undergoes a Hopf-Landau bifurcation and a two-dimensional torus with incommensurate frequencies f_0 and $f_1=0.5$ GHz appears. While f_0 is approximately the relaxation frequency of the laser, f_1 is related with the inverse of the external resonator round-trip time $f_1 \approx \tau^{-1} = (L_{ext}/2c)^{-1}$.

Figure 1a shows the Poincaré section of the torus. As the feedback k is increased, the torus period doubles three times (figs. 1b, 1c, 1d) and then becomes chaotic (fig. 1e).

The transition to the chaotic state can be recognized by power spectrum analysis. The power spectrum was calculated for the time series of the normalized photon number using 4096 sampling points and a sampling interval $dt=0.04$ ns. A series of Fourier spectra are shown in fig. 2. For $k=0.006$, the spectrum presents a typical quasiperiodic nature, where two incommensurate frequencies are present (f_0 and f_1). For $k=0.0064$, $k=0.0066$, and $k=0.00666$ the spectrum shows evidence of period doubling. In addition, for $k=0.0064$ the spectrum shows evidence of frequency locking. Increasing k, the spectrum changes to that with a broad-band noise characteristic of chaotic attractors (see fig. 2e).

4. Lyapunov analysis

The spectrum of Lyapunov exponents presents a useful tool for the study and classification of the attractors of a dynamical system [15,23]. While the positive exponents measure the expansion on the attractor, the negative exponents measure the contraction of trajectories onto the attractor. For the numerical computation of the Lyapunov exponents several algorithms available have been used [13–17]. These algorithms were compared with respect to their efficiency and accuracy for computing the Lyapunov exponents of delay equations, and the details of these investigations will reported elsewhere.

In this article the Lyapunov exponents were computed using the method proposed by Benettin et al. [13] and Shimada et al. [16]. Equations (1)–(3) were linearized but, at variance with finite dimensional problems, the linearized equations are differential delay equations: thus, we consider an infinitesimal perturbation that is not a vector with a few components, but a vector with three components, two of which (the field and the amplitude) are functions of time over the entire delay τ. The technique we used is as follows [12]: for each exponent λ_i to be computed, we selected (arbitrarily) an initial vector $dx_i(0)$. We integrated over a time τ and renormalized $dx_i(1)$ to have length one. Then, using a Gram–Schmidt algorithm, we orthonormalized the second vector relative to the first, the third relative to the first and second, and so on. We repeated this procedure for L iterations and computed

$$\lambda_i = \frac{1}{L\tau} \sum_{k=1}^{L} \log \frac{|dx_i(k)|}{|dx_i(k-1)|} . \tag{4}$$

where the euclidean metric was chosen to define distances in the phase space

$$|dx_i(k)|^2 = \sum_j dE_j^2 + \sum_j d\phi_j^2 + dN^2(k) . \tag{5}$$

Here dE_j and $d\phi_j$ are the components of the perturbations in the electric field and phase over the entire delay τ.

Equations (1)–(3) are invariant under a global translation in the phase $(\phi_j \to \phi_j + a)$. This invariance introduces a "spurious" zero Lyapunov exponent in the spectrum, since two points in the attractor that differ by a constant value of ϕ will not merge nor separate. The "extra" zero exponent will be ignored in the rest of our calculations.

Because the computation of many Lyapunov exponents is too time consuming, we computed only the ten largest Lyapunov exponents. We noted that, if we increased the number of calculated exponents, the additional exponents that appear were all negative.

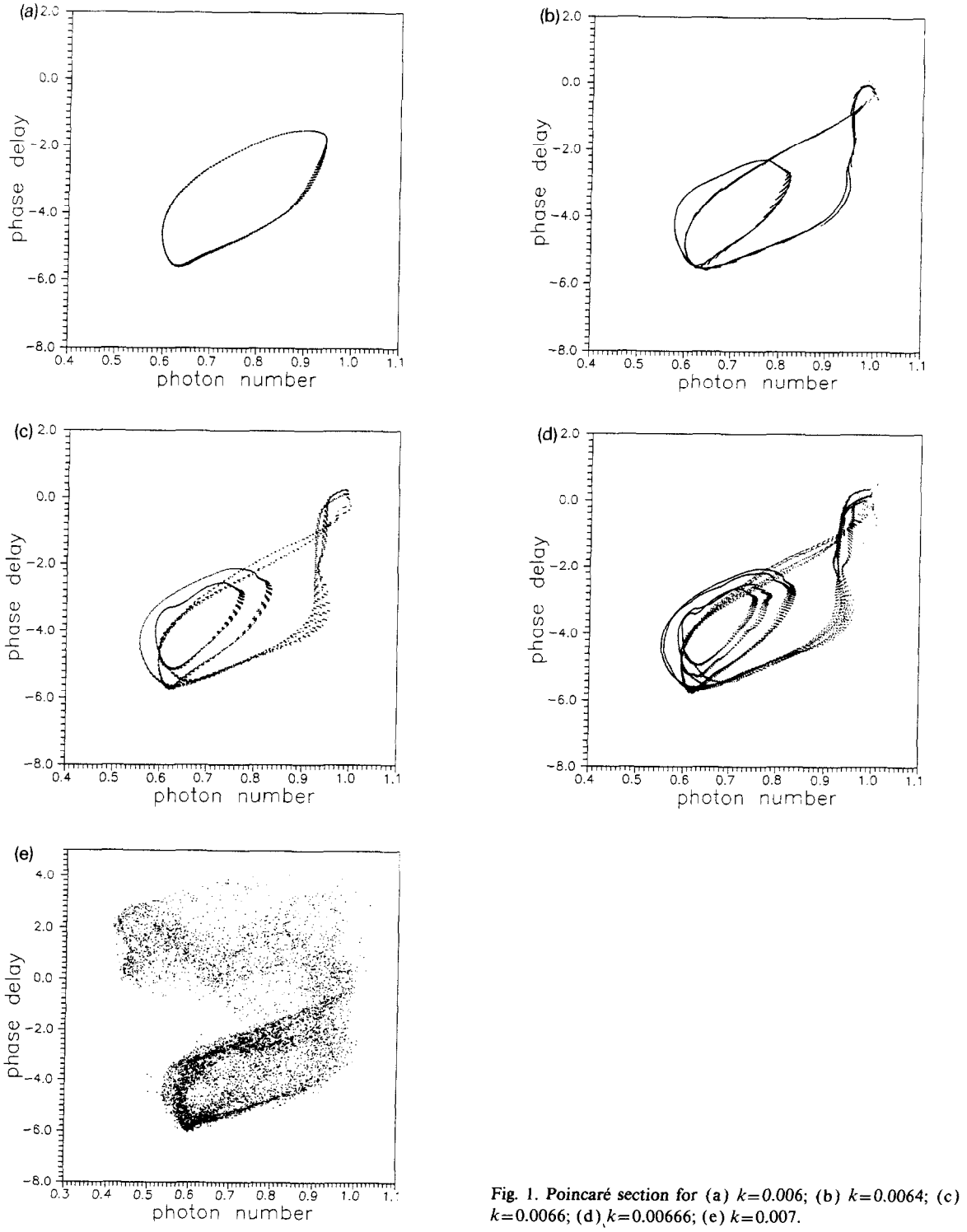

Fig. 1. Poincaré section for (a) $k=0.006$; (b) $k=0.0064$; (c) $k=0.0066$; (d) $k=0.00666$; (e) $k=0.007$.

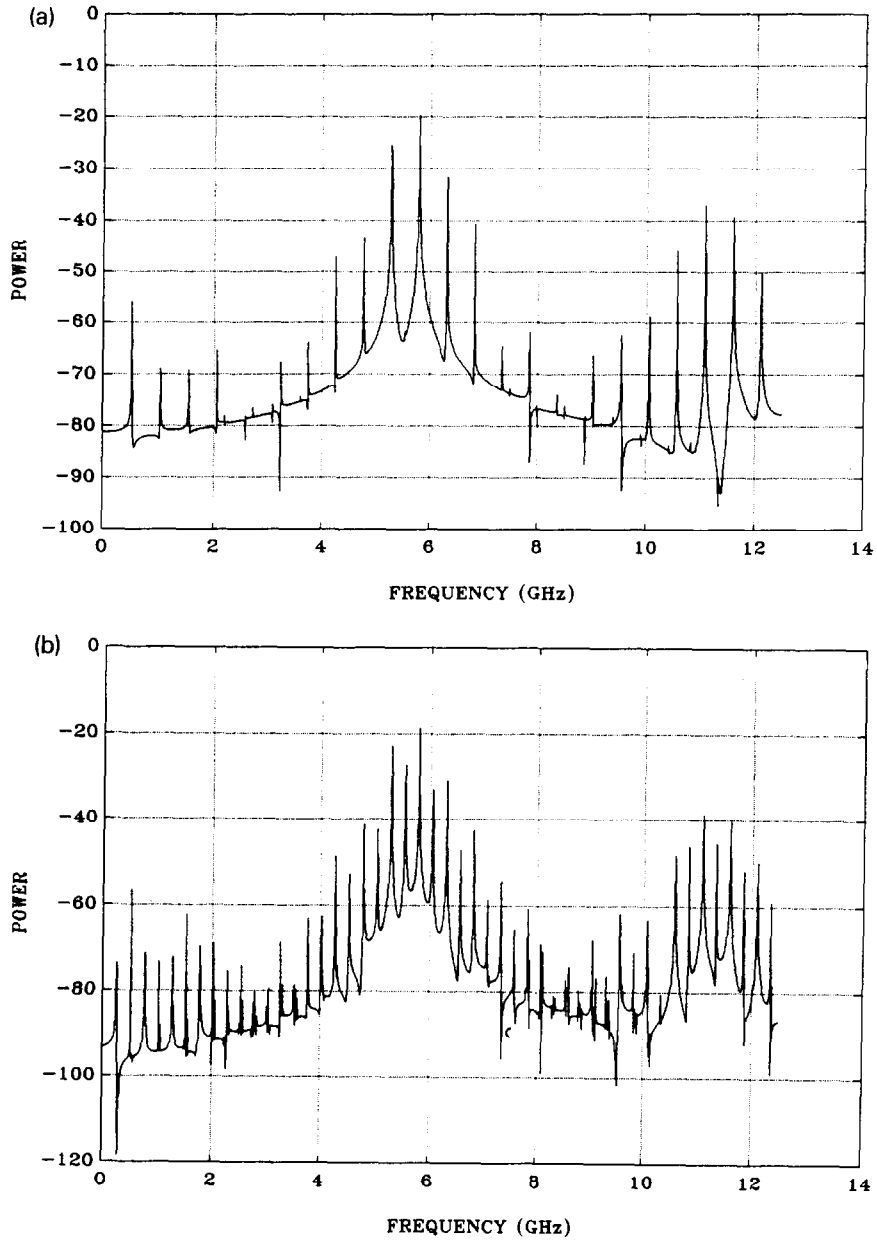

Fig. 2. Power spectra at the transition from periodicity to chaos for feedback levels of (a) 0.006; (b) 0.0064; (c) 0.0066; (d) 0.00666; (e) 0.007.

Figure 3 shows the spectrum of the five largest Lyapunov exponents as the parameter k is varied from 0.006 to 0.007. We can observe three period doubling bifurcations at $k=0.00612$, $k=0.00646$, $k=0.0664$ when the third Lyapunov exponent becomes zero, and a transition to the chaotic state at $k=0.00668$ when the first exponent becomes positive. The largest exponent of the coherence collapsed state, for $k=0.007$ was found $\lambda_1 \approx 0.12$.

The largest Lyapunov exponent was also calcu-

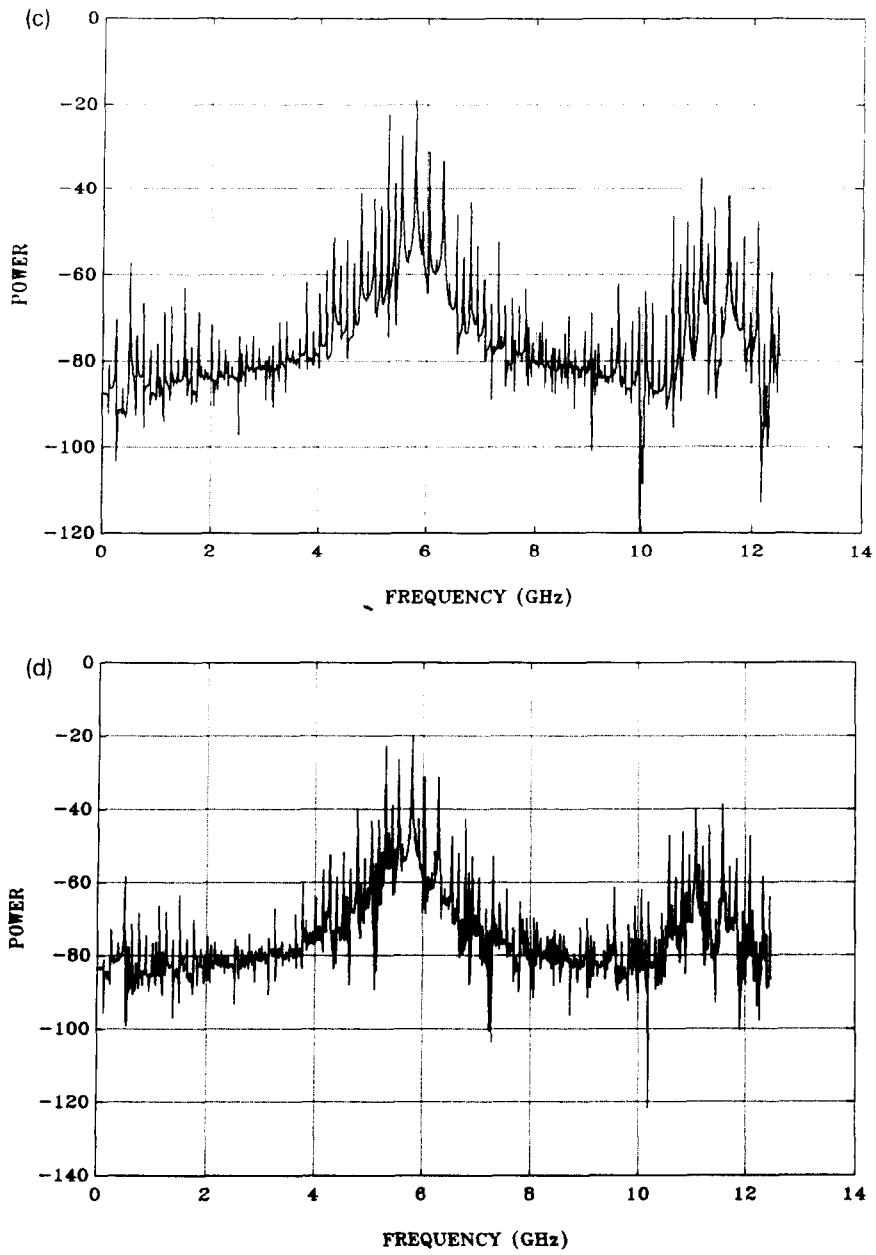

Fig. 2. Continued

lated examining the evolution of an "infinitesimally small" displacement vector $dx(0)$ at a given point on the attractor. For a chaotic system, the evolved vector $dx(t)$ grows (on average) as

$$dx(t) = dx(0)\exp(\lambda t)\,, \tag{6}$$

where $\lambda > 0$ is the largest Lyapunov exponent. Figure 4 shows the two largest Lyapunov exponents λ_1 and λ_2 calculated with eq. (4) and the largest Lyapunov exponent λ calculated with eq. (6). We observe a very good agreement between both calculations. For the

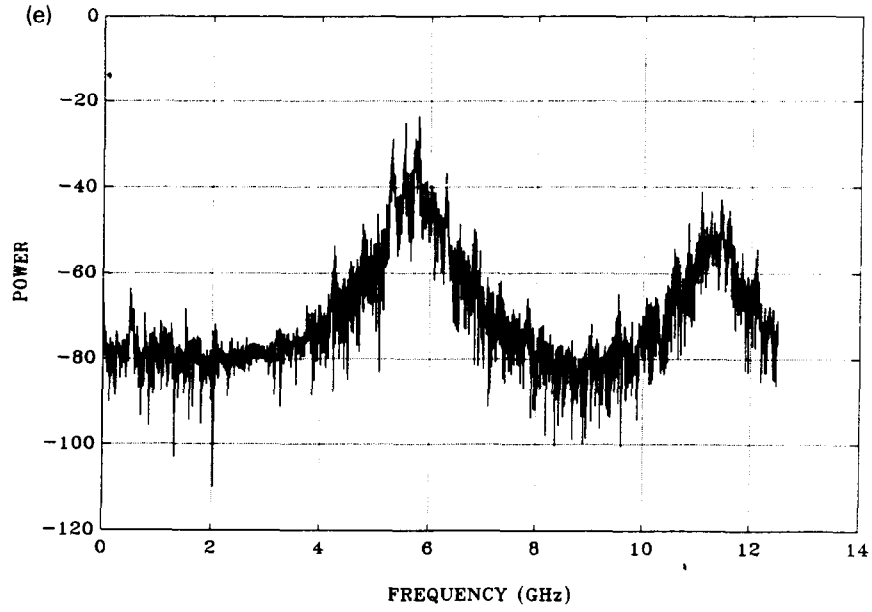

Fig. 2. Continued

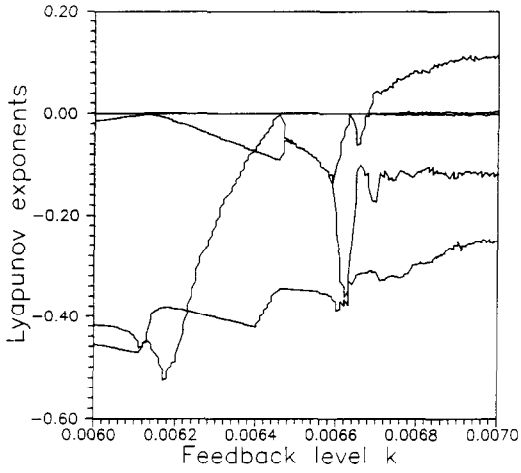

Fig. 3. The five largest Lyapunov exponents as the feedback parameter k varies from 0.006 to 0.007.

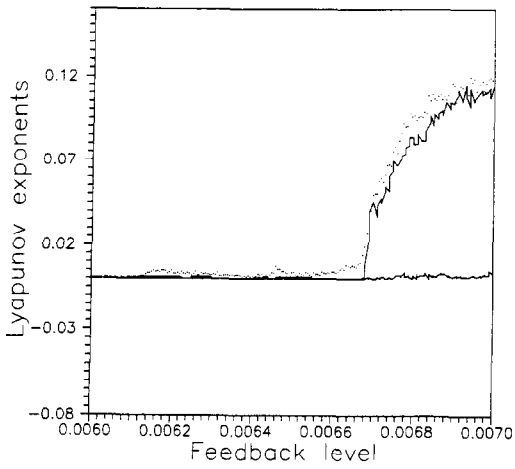

Fig. 4. The largest Lyapunov exponent calculated with eq. (6) (dotted) and the two largest Lyapunov exponents calculated with eq. (4) (solid).

coherence collapsed state ($k=0.007$) it was found $\lambda \approx 0.12$.

5. Dimension calculations

In order to arrive at a deeper understanding of the dynamics, we now turn to the calculation of the dimension of the chaotic attractor [12,23,26–28].

Since the system is infinite dimensional, both the dimension of the phase space where the attractor "lives" and the dimension of the attractor are un-

known. To recover this phase space, we used the time-difference method [18–20] applied to time series of the normalized photon number. Given the time series $x_1, x_2, \ldots x_N$, we constructed a space of high enough dimension which allows the attractor to lie there unconstrained, i.e., we form a set of d-dimensional vectors with components taken from the time series $y_i=(x_i, x_{i+p}, \ldots, x_{i+(d-1)p})$ with $i=1, \ldots, N-(d-1)p$; where d is the embedding dimension and p is the delay time.

The correlation dimension, which gives a lower bound of the fractal dimension, was calculated following the procedure of Grassberger and Procaccia [21]. The correlation function

$$C(r)=1/N^2$$

$$(\text{Number of pairs}(x_i, x_j)\text{with } |x_i-x_j|<r) \qquad (7)$$

was calculated for each embedding dimension d, and the scaling region in r for which $C(r)\approx r^{\mu}$ was located. If μ approaches a limiting value D_c as d is increased, D_c is identified as the correlation dimension. For the coherence collapsed state ($k=0.007$), fig. 5a shows logarithmic plots of the correlation function $C(r)$ with r for embedding dimension $d=5$, 10, 20, 30 and 40. The time series consisted of $N=70.000$ points, separated by a time $\Delta t=0.2$ ns. The local derivative of the curves, which better help to judge the quality of the plateau, is plotted in fig. 5b. Slopes for each embedding dimension were obtained using standard least squares regression. Observing the saturation of slopes the correlation dimension is estimated to be $D_c\approx 3.85$. However, this value is large enough to be possible affected by insufficient statistics.

In addition, from the spectrum of Lyapunov exponents, we calculated de Lyapunov dimension using the definition of Kaplan and Yorke [12,22]

$$D_L=j+(|\lambda_{j+1}|)^{-1}\sum_{i=1}^{j}\lambda_i, \qquad (8)$$

where j is the largest integer for which $\lambda_1+\ldots+\lambda_j\geq 0$. For typical attractors it has been conjectured [28] that the Lyapunov dimension is equal to the information dimension and thus gives a value $D_L\geq D_c$.

The Lyapunov dimension as a function of k is plotted in fig. 6 for k between 0.006 and 0.007. For $k<0.00668$ the attractor is a two-torus, there are two

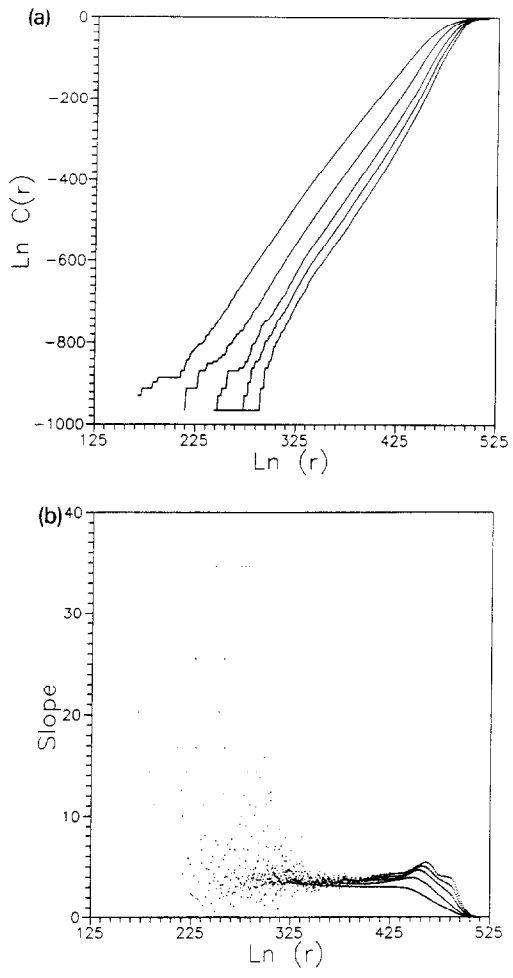

Fig. 5. (a) Doubly logarithmic plots of the correlation function with embedding dimensions $d=5$, 10, 20, 30, 40 for the coherence collapsed state ($k=0.007$). (b) Local derivative of the $\ln[C(r)]$ versus $\ln(r)$ curves plotted against $\ln(r)$. The value of the slope at the plateau is $D_c\approx 3.85$.

exponents λ_1 and λ_2 equal to zero, and the dimension is two. At $k=0.00668$ a transition to a chaotic state occurs and the dimension abruptly jumps to three. For $k>0.00668$ the dimension exceeds three and continues to increase until it approaches four. Note that the dimension exceeds three while there is only one positive exponent and two zero exponents.

In these calculations we did not consider the "spurious" zero associated to the phase invariance of eqs. (1)–(3), because it does not influence the stability and the topological properties of the attractors. The

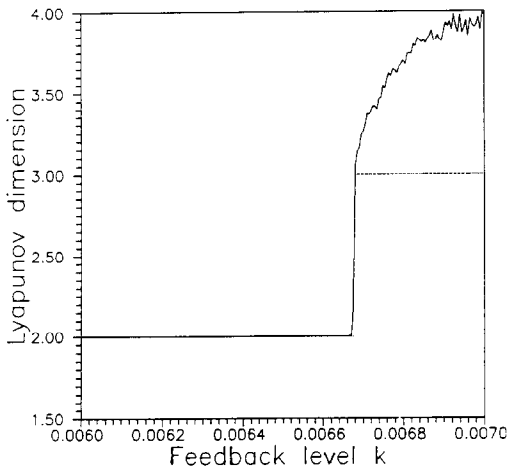

Fig. 6. The Lyapunov dimension as a function of k for $k=0.006$–0.007, calculated from eq. (8). The dimension is shown as a solid line and the number of non-negative Lyapunov exponents is indicated by a dotted line.

Lyapunov dimension of the coherence collapsed state (for $k=0.007$) gives $D_L=3.95$.

6. Conclusions and discussion

In conclusion, a detailed investigation on the properties of the coherence collapsed state has yielded a definitive identification of chaos. Dimension analysis confirms that the laser dynamics occurs in a low dimensional space, in spite of the fact that the time evolution of the laser with optical feedback depends on the field stored in the external cavity, and therefore the system has an infinite number of degrees of freedom. By Fourier and Poincaré section analysis, three period-doubling bifurcations of the torus were detected, and evidence of frequency locking was found. The spectrum of Lyapunov exponents of the coherence collapsed state confirms that the laser dynamics is highly chaotic. The details of the transition from quasiperiodicity to chaos along with the investigation of the effects of the spontaneous emission terms is in progress and will be reported elsewhere.

Acknowledgements

We would like to thank Dr. A. Lezama for bringing ref. [11] to our attention. This work was supported in part by PEDECIBA (Project URU/84/002-UNDP).

References

[1] K. Ikeda, Optics Comm. 30 (1979) 257;
K. Ikeda, H. Daido and O. Akimoto, Phys. Rev. Lett. 45 (1980) 709.
[2] D. Lenstra, B.H. Verbeek and A.J. den Boef, IEEE J. Quantum Electron. QE-21 (1985) 674.
[3] Y. Cho and T. Umeda, Optics Comm. 59 (1986) 131.
[4] G.C. Dente, P.S. Durkin, K.A. Wilson and C.E. Moeller, IEEE J. Quantum Electron. QE-24 (1988) 2441.
[5] D. Baums, W. Elsasser and E.O. Gobel, Phys. Rev. Lett. 63 (1989) 155.
[6] B. Tromborg and J. Mork, IEEE J. Quantum Electron. QE-26 (1990) 642.
[7] J. Sacher, W. Elsässer and E.O. Gobel, IEEE J. Quantum Electron. 27 (1991) 373.
[8] R. Lang and K. Kobayashi, IEEE J. Quantum Electron. QE-16 (1980) 347.
[9] B. Tromborg, J.H. Osmundsen and H. Olesen, IEEE J. Quantum Electron. QE-20 (1984) 1023.
[10] B. Tromborg and J. Mork, Photon. Technol. Lett. 2 (1990) 549.
[11] J. Mork, J. Mark and B. Tromborg, Phys. Rev. Lett. 65 (1990) 1999.
[12] J.D. Farmer, Physica D 4 (1982) 366.
[13] G. Benettin, L. Galgani and J.-M. Strelcyn, Phys. Rev. A 14 (1976) 2338.
[14] J.P. Eckmann and D. Ruelle, Rev. Mod. Phys. 57 (1985) 617.
[15] H. Bai-Lin, Chaos II (World Scientific, Singapore, 1990).
[16] I. Shimada and T. Nagashima, Prog. Theor. Phys. 61 (1979) 1605.
[17] A. Wolf, J.B. Swift, H.L. Swinney and J.A. Vastano, Physica D 16 (1985) 285.
[18] N.H. Packard, J.P. Crutchfield, J.D. Farmer and R.S. Shaw, Phys. Rev. Lett. 45 (1980) 712.
[19] F. Takens, in: Lecture notes in mathematics, No. 989, eds. D.A. Rand and L.S. Young (Springer, Berlin, 1981).
[20] T.S. Parker and L.O. Chua, Proc. IEEE 75 (1987) 982; Practical Numerical algorithms for chaotic systems (Springer, Berlin, 1989).
[21] P. Grassberger and I. Procaccia, Phys. Rev. Lett. 50 (1983) 346.
[22] J. Kaplan and J. Yorke, Functional differential equations and approximation of fixed points, eds. H.O. Peitgen and H.O. Walther (Springer, Berlin, 1979) p. 228.

[23] H.G. Schuster, Deterministic chaos (VCH, Weinheim, 1988).
[24] A. Arneodo, P.H. Coullet and E.A. Spiegel, Phys. Lett. A 94 (1983) 1.
[25] K. Kaneko, Collapse of tori and genesis of chaos in dissipative systems (World Scientific, Singapore, 1986).
[26] P. Bergé, Y. Pomeau and C. Vidal, Order within chaos (Hermann, Paris, 1984).
[27] H. Bai-Lin, Elementary symbolic dynamics (World Scientific, Singapore, 1989).
[28] J.D. Farmer, E. Ott and J.A. Yorke, Physica D 7 (1983) 153.